Face Recognition Based on LBP Multi-feature Extraction Fusion and KNN

Huiyan Liu[1]

Artificial Intelligence College, Shenyang Normal University
Shenyang, 110034 China
Received May. 28, 2025; Revised and Accepted July. 7, 2025

Abstract. The widespread application of facial recognition technology has enriched people's digital lives. In such a digital age, data intelligence based on cognitive computing has transformed an individual from a statistically average person into an object that can be analyzed for data independently. This change heralds the arrival of a data analysis society. The facial recognition system integrates multiple professional technologies such as artificial intelligence, machine recognition, machine learning, model theory, expert systems, and video image processing. At the same time, it needs to combine the theory and implementation of intermediate value processing, and is the latest application of biometric recognition. The realization of its core technology demonstrates the transformation from weak artificial intelligence to strong artificial intelligence. To effectively extract facial features from different angles and postures under complex lighting conditions, this paper proposes a novel LBP multi-feature extraction fusion and KNN method. This paper proposes two improved local binary patterns (LBP), namely weighted fusion of triangular features with local binary pattern (WLBP) and Tulapuras local binary pattern (TLBP). They are fused with the Gabor filter and then classified by using the KNN classifier. The experiment adopts the YALEB, ORL and FERET face databases to conduct experiments. The experimental results show that the proposed method significantly improves the accuracy of face recognition under complex lighting and multi-angle and pose conditions compared with the traditional single LBP method.

Keywords: Facial recognition, Local binary patterns, KNN, Gabor filter.

1. Introduction

Facial recognition technology, as a key branch of biometric identification, plays a significant role in multiple fields such as security verification, monitoring systems, and intelligent interaction [1]. In recent years, researchers have proposed many face recognition algorithms, such as Scale-Invariant Feature Transform (SIFT) [2], Accelerated Robust Features (SURF) [3], etc,. However, these methods are limited in recognizing faces of different angles and postures under complex lighting conditions and have high computational complexity. Local Binary Pattern (LBP), as a classic texture feature descriptor, is widely used in the field of image recognition due to its simple calculation [4-6]. Many variants of LBP have also been proposed, such as CS-LBP [7], LCCP [8], LCCMSP [9], etc. However, there are also some problems. It may improve lighting and rotation, but its basic framework still has not completely solved the complexity of image variability in CS-LBP. CS-LBP has certain advantages in local features, but because it only relies on binarized features, it is relatively simplified, and lacks strong robustness when there are significant changes in rotation, scale, lighting, etc. In addition, Gabor features, with their excellent time-frequency characteristics, have also been widely applied in face recognition [10].

Based on this, this paper proposes a multi-feature fusion feature extraction algorithm that combines improved LBP and Gabor features. Firstly, the expression ability of image texture and edge information is enhanced by introducing the WLBP and TLBP. Secondly, Gabor filter is utilized to extract multi-scale and multi-directional features of the image to obtain more comprehensive feature information. Finally, the improved LBP features are fused with Gabor features. Through the complementarity of multiple features, the effective extraction of facial features from different angles and postures under complex lighting conditions is enhanced. The experimental results show that this method has achieved a high recognition accuracy rate on multiple complex lighting and face datasets with different angles and postures, verifying its effectiveness and superiority in the field of face recognition.

2. Proposed Face Recognition Method

2.1. LBP

Local Binary Pattern (LBP) is texture descriptors widely used in the fields of image processing and computer vision. The basic principle of LBP is to compare the gray values of 8 adjacent pixels within a 3×3 window, with

the central pixel of the window as the threshold. If the around pixel values are greater than those in the center, the position is marked as 1; otherwise, it is marked as 0. In this way, an 8-bit binary number can be obtained [11,12]. This value is used as the LBP value of the pixel at the center of the window to reflect the texture information of this 3×3 area. The principle is shown in figure 1.

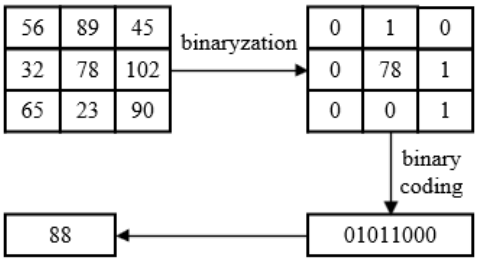

Fig. 1. LBP process

$$LBP(x_c, y_c) = \sum_{i=1}^{8} 2^{i-1} f(g_i - g_c). \tag{1}$$

Where (x_c, y_c) represents the position of the central pixel of LBP. g_c represents the gray value of the central pixel point. g_i represents the gray value of the neighboring pixel points. $f(x)$ is a binary function, defined by the following formula.

$$f(x) = 1, x \geq 0. \tag{2}$$

2.2. WLBP

The traditional LBP relies on a simple binary comparison of the central pixel of the image and its neighboring pixels, which leads to sensitivity to illumination changes and inability to effectively handle rotational invariance, limiting its application in complex image analysis. When dealing with images, fixed weights or simple rules are usually adopted, lacking flexible adaptability. The weighted fusion local binary pattern algorithm for triangular features forms multiple triangles by selecting different combinations of neighboring pixels, and enhances the capture of angular information and spatial relationships in the image through the geometric characteristics of the triangles [13,14]. During the feature extraction process, the algorithm designs a multiple weighting mechanism, that is, cosine weights and Gaussian smoothing weights are used to smooth the angular relationship between neighboring pixels and enhance the robustness against rotation. The adaptive weight based on matrix features dynamically adjusts the feature weights by introducing the ratio of trace, norm and condition number, so as to endow different regions with different feature contribution degrees and better handle illumination changes.

Specifically, trace values enable the overall strength of local features in an image to be effectively evaluated, which can help the system focus on areas with stronger texture information. The norm value enhances the recognition of complex textures or structural regions, helping the system better locate important features in complex images. The condition number provides a sensitivity measure for image stability and noise, helping the system balance stability and complexity in the image and avoid the interference of noise. The geometric characteristics of each triangle are ultimately weighted and summed to form a feature matrix containing local triangle texture information, significantly improving the expression ability of complex textures. The algorithm flow is shown in Figure 2.

By combining the triangular geometric structure and matrix features, this algorithm has both local sensitivity and global stability in texture expression, and can describe the complex texture patterns in images more effectively. The core step formula is as follows:

1. The Area of a triangle is calculated based on the row-column difference of the pixel neighborhood coordinates.

$$Area = \left\| \begin{matrix} 1 & 1 & 1 \\ r_c & r_1 & r_2 \\ c_c & c_1 & c_2 \end{matrix} \right\| \tag{3}$$

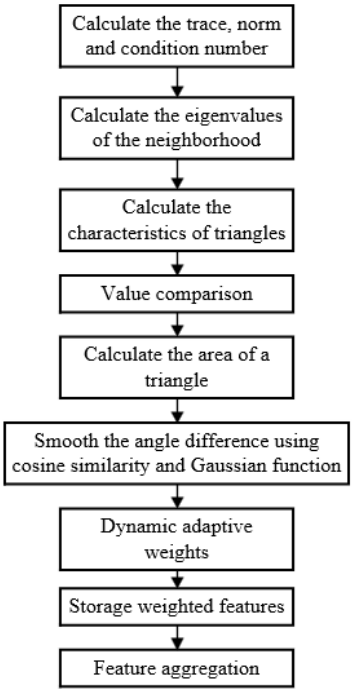

Fig. 2. WLBP process

Where, r_c and c_c are the row and column coordinates of the central pixel. (r_1, c_1) and (r_2, c_2) are the row and column coordinates of two neighboring pixels. $Area$ measures the degree of dispersion of pixel distribution in the neighborhood. A large area indicates that the distribution of neighborhood points is relatively far away.

2. Value comparison. By comparing the central pixel value $I(r_c, c_i)$ with the neighboring pixel values $I(r_i, c_i)$, a Boolean value comparison is generated.

$$valueComparison = \begin{cases} 1 = & I(r_i, c_i) > I(r_c, c_c) \\ 0 = & otherwise \end{cases} \tag{4}$$

3. Calculating the cosine similarity weight, Gaussian function smoothing Angle difference weight and dynamic adaptive weight.

$$cosWeight = 1 + cos(anglesDiff(i)). \tag{5}$$

$$gassWeight = exp(-\frac{anglesDiff(i)^2}{2\sigma^2}). \tag{6}$$

$$traceWeight = \frac{traceVal}{traceVal + normVal + \alpha}. \tag{7}$$

$$normWeight = \frac{normVal}{traceVal + normVal + \alpha}. \tag{8}$$

$$condWeight = \frac{conditionNum}{conditionNum + \alpha}. \tag{9}$$

Here, $anglesDiff$ is the Angle difference between the current pixel and its neighbors. $cosWeight$ is the cosine similarity weight. $gassWeight$ is the smoothing Angle difference weight of the Gaussian function. σ is the standard deviation of the Gaussian function. α is a small constant used to prevent division by zero. $traceWeight$ is the trace weight. $traceVal$ is the trace of the neighborhood matrix. $normVal$ is the norm of the neighborhood matrix. $normWeight$ is the norm weight. $condWeight$ is the weight of the condition number. $conditionNum$ is a condition number.

4. Weighted eigenvalue. The comparison results of the values, areas and weights of each triangle are comprehensively calculated.

$$triangleFeature(k) = \sum_{i=1}^{8}(valueComparison \cdot Area_i \cdot cosWeight \cdot gassWeight_i \cdot WeightType_k). \quad (10)$$

Where $k \in 1, 2, 3, 4$ corresponds to trace, norm, condition number and sum.

5. Feature aggregation. Sum up the eigenvalues of all triangles to obtain the feature of pixel $I(r, c)$.

$$Feature(r, c) = \sum_{k=1}^{4} triangleFeatures(k). \quad (11)$$

2.3. TLBP

Local Binary Pattern (LBP) relies on local comparisons between pixel values, ignoring the spatial structure and directionality between neighboring pixels, which makes it underperform when dealing with images with complex textures or directionality changes. Secondly, LBP is highly sensitive to noise, especially in images with low contrast or high noise levels. Even minor gray scale changes can lead to incorrect binary patterns, thereby affecting the stability and accuracy of features [15-17].

To address these deficiencies, we introduce graph Laplacian features to provide a more comprehensive texture description based on the traditional LBP, the Graph Laplacian local binary pattern. Specifically, it models the similarity between neighboring pixels by constructing an adjacency matrix, which not only takes into account the differences in pixel values but also integrates directional weights, enabling features to better capture directional texture and structural information. Furthermore, the Laplacian matrix feature of this algorithm does not merely rely on the gray-level differences of neighboring pixels, but also quantifies the global connectivity of the neighborhood structure through the spectral characteristics (the sum of eigenvalues) of the adjacency matrix and the Laplacian matrix. This approach differs from the traditional Laplacian filtering method based on image gradients. By introducing spectral features, it can more accurately reflect the geometric structure and texture relationship of local regions in the image, thereby enhancing the algorithm's ability to capture details. The algorithm flow is shown in Figure 3.

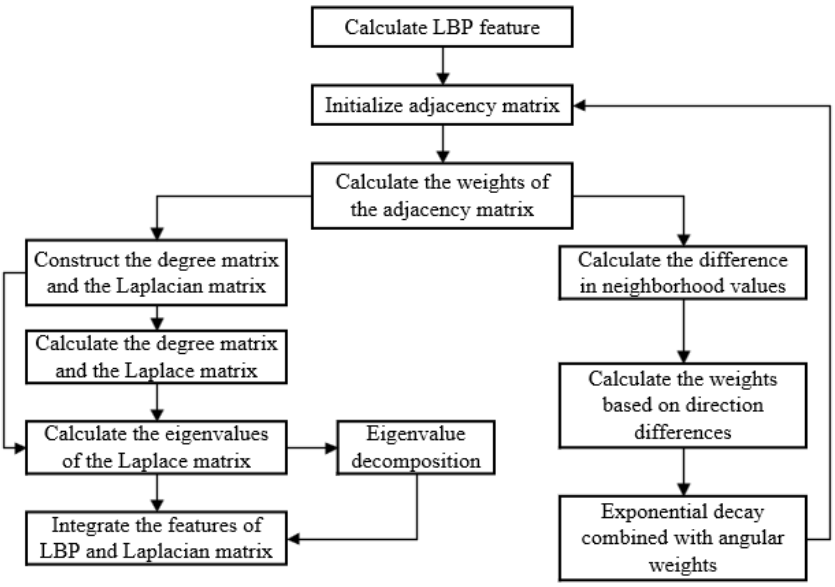

Fig. 3. TLBP process

The calculation steps are as follows.

1. Calculate the LBP feature and the weight of the adjacency matrix.

$$A_{ij} = exp(-|I(r_i, c_i) - I(r_j, c_j)|) \times (1 - |\cos(\theta_i - \theta_j)|). \tag{12}$$

Where, $|I(r_i, c_i) - I(r_j, c_j)|$ represents the absolute difference of the neighboring pixel values, reflecting the similarity between pixel values. $1-|\cos(\theta_i-\theta_j)|$ is a directional weighting that reflects the relative difference in direction between two neighboring points.

2. Degree matrix.

$$D = diag(\sum_{j=1}^{8} A_{ij}). \tag{13}$$

3. Laplacian matrix.

$$L = D - A. \tag{14}$$

It calculates the eigenvalues $(\lambda_1, \cdots, \lambda_8)$ of the Laplacian matrix through eigenvalue decomposition.

$$Laplacian(r, c) = \sum_{i=1}^{8} \lambda_i. \tag{15}$$

4. Feature value fusion.

2.4. Gabor Filter

The principle of Gabor filters in image recognition is based on their ability to simulate the characteristics of the human visual system. By applying Gabor functions at different scales and directions, they capture local features in images, such as edges, corners, and textures [18]. This multi-scale and multi-directional characteristic enables the Gabor filter to effectively describe the texture information in the image, and it has strong robustness against changes in brightness, contrast, and image pose. The local features extracted by the Gabor filter, including frequency and direction information, provide rich information for image recognition. Moreover, due to its sensitivity to local changes, it performs well in edge detection and texture analysis. In addition, normalization processing of Gabor features helps to reduce the computational load and improve the accuracy of recognition [19,20]. Therefore, Gabor filters have been widely applied in the field of image recognition due to their advantages in simulating human visual texture recognition and extracting local features of images.

$$\psi(x, y) = \frac{1}{2\pi\sigma^2} e^a e^b. \tag{16}$$

Where $x' = x\cos\theta + y\sin\theta$, $y' = -x\sin\theta + y\cos\theta$. $a = -\frac{x'^2 + r^2 y'^2}{2\sigma^2}$, $b = j2\pi\frac{x'}{\lambda} + \psi$. σ is the standard deviation of the Gaussian function. r is the aspect ratio. λ is the wavelength of a sine wave. θ is the direction of the filter. ψ is the phase shift.

2.5. KNN Based on Mean Feature Vector of the Training Set

As a parameter-free classification method, the traditional KNN algorithm performs well in machine learning based on statistical features, but it also has some drawbacks [21]. First, handwritten digit images have high-dimensional features. For the entire image, the extracted LBP feature vector is 256 dimensions, and for a four-partition image, the combined LBP feature vector extracted is 1024 dimensions, making the operation rather complex. Second, the handwritten number samples of different people vary greatly, resulting in a large distance between sample points within the same category [22,23]. This may lead to many sample points from other categories in the training set entering the k-nearest range, causing model judgment errors. This paper proposes an improved KNN algorithm based on the mean feature vector of the training set. The algorithm steps are as follows.

Step 1. For $m \times n$ training set images with class m, the images are partitioned, and the LBP feature vectors after partitioning are extracted respectively. Then, the LBP feature vectors after partitioning are combined to form the feature vector x_{gi} of the image sample. Among them, the two-dimensional LBP feature vector of the $i-th$ sample of the $g-th$ class is represented as $x_{gi} = (a_{gi1}, a_{gi2}, \cdots, a_{giz})$. a_{gij} represents the $j-th$ eigenvalue of this image.

Step 2. For all sample points of class g, it finds the mean eigenvector $x_g = (\bar{a}_{g1}, \bar{a}_{g2}, \cdots, \bar{a}_{gz})$ as the representative feature point. The calculation formula is shown as follows.

$$\bar{x}_g = \frac{\sum_{1 \le i \le n} x_{gi}}{n}. \tag{17}$$

$$\bar{a}_{gj} = \frac{\sum_{1 \le i \le n} a_{gij}}{n}. \tag{18}$$

It performs the same operation on all categories to obtain m mean feature vectors, which are then used to form the training set feature matrix, as shown in equation (19).

$$U = [\bar{x_1}, \bar{x_2}, \cdots, \bar{x_m}]^T. \tag{19}$$

Step 3. Using the calculated feature matrix, the KNN algorithm with $K = 1$ is adopted for training, and the test set is predicted to observe the classification results.

The improved KNN algorithm only needs to determine the distance between the LBP feature vector of the newly input unknown sample and the m mean feature vectors. At this time, each category is represented by only one feature vector, so K is selected as 1, eliminating the reduction in classification accuracy caused by excessive differences among samples of the same category and inappropriate selection of K values. Since the input sample size m of the improved KNN algorithm is much smaller than the sample quantity $m \times n$, the computational load can be reduced.

3. Experimental Procedures and Result Analysis

3.1. Face Database

This paper calculates the recognition rate under three face databases, namely YALEB, ORL and FERET, based on the characteristics of some face databases. The images in the YALEB face database were collected from 64 different light source angles, covering conditions from frontal illumination to extreme side illumination, which can test the effectiveness of the algorithm under complex lighting conditions. The ORL face database images include frontal and slight side views, different expressions (such as smiling and expressionless), and those with and without glasses, which can be used to test the effectiveness of the algorithm at different angles. The FERET database contains a large number of face images, covering features such as different ages, genders, races, hairstyles, and glasses. Its core feature is that it includes multiple shooting angles, different lighting conditions, and various pose variations, thus having high complexity. It can test the effectiveness of algorithms in multiple angles and poses under complex lighting conditions. It is a synthesis of the first two database conditions. The specific experimental data are shown in Table 1.

Table 1. Detailed experimental data from various databases

Database	Class number	Sample number of each type	Total sample	Training number	Testing	Pixel
YALEB	38	64	2432	32	32	64×64
ORL	40	10	400	5	5	64×64
FERET	200	7	1400	5	2	80×80

3.2. Recognition Rates Under Different Blocks

The size of the blocks has a significant connection with the recognition rate of the image. If the blocks are too large, the image correlation cannot be reflected; if they are too small, some important image features may be lost [4]. To verify whether the proposed algorithm in this paper has more advantages under different blocks. The experiment first calculates the recognition rates of the TLBP and WLBP algorithms respectively under 1×1, 2×2, and 4×4 blocks, and then performs histogram fusion with Gabor under the block with the highest recognition rate. This paper conducts experiments using the KNN classifier. Random forest is an ensemble learning method, which builds multiple decision trees and combines their prediction results to improve the performance and accuracy of the overall model. Each decision tree in KNN is a classifier. They are independently trained on the data and vote on the result when making the final prediction.

From Tables 2, 3 and 4, we can see that the recognition rates of the TLBP and WLBP algorithms using the KNN classifier under different blocks on the YALEB, ORL and FERET face databases are much higher than those of the LBP algorithm. Based on the recognition rate results, we respectively select 4×4, 4×4, and 2×2 blocks to combine with Gabor. It can be seen from the results in Table 5 that the recognition rate of the fused algorithm is also higher than that of the single algorithm.

Table 2. Experiment result on YALEB with KNN

Method	1×1	2×2	4×4
LBP	0.5338	0.8488	0.9837
TLBP	0.5922	0.8776	0.9861
WLBP	0.5634	0.8916	0.9919

Table 3. Experiment result on ORL with KNN

Method	1×1	2×2	4×4
LBP	0.7551	0.8651	0.9051
TLBP	0.8051	0.8851	0.9601
WLBP	0.8101	0.9051	0.9651

Table 4. Experiment result on FERET with KNN

Method	1×1	2×2	4×4
LBP	0.2851	0.4226	0.4976
TLBP	0.4801	0.6426	0.6251
WLBP	0.5576	0.6276	0.6551

3.3. Recognition Rates with Different classifiers

Furthermore, to verify the performance under different classifiers, the YALEB face dataset is re-partitioned under both SVM and KNN classifiers to calculate the recognition rate, and the fusion algorithm is compared with a single algorithm. The recognition rate results are shown in Tables 6 and 7. It can be seen that good results are maintained under different classifiers.

3.4. Comparison with Other Methods

The recognition rate of a system is an important indicator for measuring its performance. The new method in this paper is compared with the following five methods on three face databases. As can be seen from Table 8, the proposed algorithm in this paper has certain advantages over both the traditional single LBP variant algorithm and some current feature fusion algorithms.

In this study, we first verified that two improved local binary pattern algorithms, TLBP and WLBP, outperform the traditional LBP algorithm in feature extraction when dealing with complex lighting conditions and multi-angle and pose changes by calculating recognition rates on multiple face databases. Secondly, by applying KNN classifiers on different face databases and calculating the recognition rate, we further demonstrated the significant improvement in recognition accuracy of the multi-feature fusion algorithm compared to the single feature extraction method. Finally, we applied multiple classifiers on the YALEB face database to calculate the recognition rate in order to evaluate the stability of the algorithm under different classifiers. These results not only confirm the effectiveness of the improved LBP algorithm in extracting facial features on complex lighting and multi-angle and multi-pose face datasets, but also demonstrate the superiority of the multi-feature fusion strategy in face recognition tasks.

Table 5. WLBP, TLBP and Gabor fusion under the optimal partitioning

Method	YALEB	ORL	FERET
Gabor	0.8809	0.9351	0.3501
WLBP+TLBP+Gabor	0.9935	0.9701	0.7176

Table 6. YALEB (RF, SVM, KNN)

Method	RF	SVM	KNN
LBP	0.9836	0.8241	0.9697
TLBP	0.9861	0.9368	0.9771
WLBP	0.9919	0.9326	0.9763

4. Conclusion

Based on the existing feature extraction operator LBP, this paper improves and applies two new feature extraction algorithms, WLBP and TLBP, and extracts the Gabor features of the image, using multi-feature fusion for face classification. Through the analysis of the experimental results, the proposed algorithm shows a high recognition rate and good performance in all three face datasets. Next, we plan to conduct research in the following several directions.

1. This paper uses direct histogram concatenation and fusion, which may bring redundant information and affect the classification results. More effective fusion methods will be selected in the future.
2. The dataset is relatively small in scale. In future work, we plan to evaluate the method proposed in this paper under more complex datasets and classifiers, and extend it to other challenging computer vision applications.
3. The method proposed in this paper only focuses on facial features of multiple angles and postures under complex lighting conditions. No experiments have been conducted on other external redundant information that may affect the extraction of feature information. Experiments will be considered in other complex environmental conditions later.

5. Conflict of Interest

The authors declare that there are no conflict of interests, we do not have any possible conflicts of interest.

Acknowledgments. None.

References

1. Rinaldi T, Valle A. Decision-making and justice: unraveling the threads of social equity[C]//Proceedings of the Third International Conference of the journal Scuola Democratica. Education and/for Social Justice. Vol. 1: Inequality, Inclusion, and Governance. Associazione "Per Scuola Democratica", 2025: 1081-1086.
2. Burger W, Burge M J. Scale-invariant feature transform (SIFT)[M]//Digital Image Processing: An Algorithmic Introduction. Cham: Springer International Publishing, 2022: 709-763.
3. Bay H, Ess A, Tuytelaars T, et al. Speeded-up robust features (SURF)[J]. Computer vision and image understanding, 2008, 110(3): 346-359.
4. Hu S, Li J, Fan H, et al. Scale and pattern adaptive local binary pattern for texture classification[J]. Expert Systems with Applications, 2024, 240: 122403.
5. Fadaei S, Dehghani A, Ravaei B. Content-based image retrieval using multi-scale averaging local binary patterns[J]. Digital Signal Processing, 2024, 146: 104391.
6. Yin N, Sun Y, Kim J S. A CNN-Based Indoor Positioning Algorithm for Dark Environments: Integrating Local Binary Patterns and Fast Fourier Transform with the MC4L-IMU Device[J]. Applied Sciences, 2025, 15(7): 4043.

Table 7. The recognition rate of fusion under different classifiers

Method	RF	SVM	KNN
Gabor	0.8809	0.8661	0.9228
WLBP+TLBP+Gabor	0.9935	0.9375	0.9911

Table 8. Comparison with other methods

Method	YALEB	ORL	FERET
LCCP	0.8351	0.8356	0.2026
CSLBP	0.9101	0.9516	0.6276
CSLDP	0.8851	0.8849	0.4751
Reference [24]	0.9456	0.9877	0.6475
Reference [25]	0.9251	0.9893	0.4875
Proposed	0.9701	0.9935	0.7076

7. Junding S, Shisong Z, Xiaosheng W. Image retrieval based on an improved CS-LBP descriptor[C]//2010 2nd IEEE international conference on information management and engineering. IEEE, 2010: 115-117.
8. Yang Y, Duan F, Jiang J, et al. Robust method for interest region description based on local intensity binary pattern[J]. Journal of Electronic Imaging, 2017, 26(4): 043025-043025.
9. Hu M, Yang C, Zheng Y, et al. Facial expression recognition based on fusion features of center-symmetric local signal magnitude pattern[J]. IEEE Access, 2019, 7: 118435-118445.
10. Tuncer T, Dogan S. Pyramid and multi kernel based local binary pattern for texture recognition[J]. Journal of Ambient Intelligence and Humanized Computing, 2020, 11: 1241-1252.
11. Harianto E S, Setiawan B C, Prasetyo S Y, et al. Leveraging Eager Learning for Retinal Abnormality Classification with Local Binary Pattern Features[C]//2025 International Conference on Advancement in Data Science, E-learning and Information System (ICADEIS). IEEE, 2025: 1-6.
12. Finke M, Dmitrienko A. Time-Aware Face Anti-Spoofing with Rotation Invariant Local Binary Patterns and Deep Learning[C]//IFIP International Conference on ICT Systems Security and Privacy Protection. Springer, Cham, 2025: 263-277.
13. Yin W, Zhao W, You D, et al. Local binary pattern metric-based multi-focus image fusion[J]. Optics & Laser Technology, 2019, 110: 62-68.
14. Kayhan N, Fekri-Ershad S. Content based image retrieval based on weighted fusion of texture and color features derived from modified local binary patterns and local neighborhood difference patterns[J]. Multimedia Tools and Applications, 2021, 80(21): 32763-32790.
15. Ying Z, Cai L, Gan J, et al. facial expression recognition with local Binary pattern and Laplacian Eigenmaps[C]//Emerging Intelligent Computing Technology and Applications: 5th International Conference on Intelligent Computing, ICIC 2009, Ulsan, South Korea, September 16-19, 2009. Proceedings 5. Springer Berlin Heidelberg, 2009: 228-235.
16. Metin S, Dogan S. Novel Fuzzy Kernels Based Local Binary Pattern And Local Graph Structure Methods[J]. Turkish Journal of Science and Technology, 2021, 16(1): 163-177.
17. Yang B, Li Q. Local binary pattern-based discriminant graph construction for dimensionality reduction with application to face recognition[J]. Multimedia Tools and Applications, 2019, 78(16): 22445-22462.
18. Omar S S, Ahmed W S, Ismail M N, et al. In-Depth Examination of a Fingerprint Recognition System Using the Gabor Filter[C]//2024 35th Conference of Open Innovations Association (FRUCT). IEEE, 2024: 532-543.
19. de Andrade J V R, Freire A, Pereira G C, et al. Towards Robust Facial Recognition: Gabor Filter-Based Feature Extraction for NIR-VIS Heterogeneous Face Recognition[C]//Proceedings of the 40th ACM/SIGAPP Symposium on Applied Computing. 2025: 1275-1281.
20. Aliradi R, Ouamane A. A novel descriptor (LGBQ) based on Gabor filters[J]. Multimedia Tools and Applications, 2024, 83(4): 11669-11686.
21. Xie J, Xiang X, Xia S, et al. MGNR: A multi-granularity neighbor relationship and its application in KNN classification and clustering methods[J]. IEEE Transactions on Pattern Analysis and Machine Intelligence, 2024.
22. Tian G, Wang J, Wang R, et al. A multi-label social short text classification method based on contrastive learning and improved ml-KNN[J]. Expert Systems, 2024, 41(7): e13547.
23. Gong L H, Ding W, Li Z, et al. Quantum k-nearest neighbor classification algorithm via a divide-and-conquer strategy[J]. Advanced Quantum Technologies, 2024, 7(6): 2300221.
24. Tayubi I A, Pawar D N, Kiran A, et al. Facial Emotion Recognition Using a Local Binary Pattern based Deep Learning[C]//2024 2nd International Conference on Computer, Communication and Control (IC4). IEEE, 2024: 1-7.
25. Safarov F, Kutlimuratov A, Khojamuratova U, et al. Enhanced AlexNet with Gabor and Local Binary Pattern Features for Improved Facial Emotion Recognition[J]. Sensors, 2025, 25(12): 3832.